NH3 Mediated or Ion Migration Reaction: The Case Study on Halide–Amide System

ARTICLE *in* THE JOURNAL OF PHYSICAL CHEMISTRY C · JANUARY 2014

Impact Factor: 4.77 · DOI: 10.1021/jp411551v

8 AUTHORS, INCLUDING:

Hujun Cao
Chinese Academy of Sciences
13 PUBLICATIONS **47** CITATIONS
SEE PROFILE

Han Wang
Chinese Academy of Sciences
8 PUBLICATIONS **25** CITATIONS
SEE PROFILE

Jie Shan Qiu
Dalian University of Technology
423 PUBLICATIONS **7,244** CITATIONS
SEE PROFILE

THE JOURNAL OF PHYSICAL CHEMISTRY C

Article

pubs.acs.org/JPCC

NH_3 Mediated or Ion Migration Reaction: The Case Study on Halide−Amide System

Hujun Cao,[†,‡,§] Jianhui Wang,[†] Yongshen Chua,[†] Han Wang,[†,§] Guotao Wu,[†] Zhitao Xiong,[†] Jieshan Qiu,[‡] and Ping Chen*[,†]

[†]Dalian National Laboratory for Clean Energy, Dalian Institute of Chemical Physics, Chinese Academy of Sciences, Dalian 116023, P. R. China

[‡]Carbon Research Laboratory, Liaoning Key Lab for Energy Materials and Chemical Engineering, State Key Lab of Fine Chemicals, Dalian University of Technology, Dalian 116024, P. R. China

[§]University of Chinese Academy of Sciences, Beijing 100049, P. R. China

Supporting Information

ABSTRACT: Lively debates on hydrogen desorption from the amide−hydride system via either ion migration or NH_3 mediated mechanisms have been ongoing since the discovery of the amide−hydride system for hydrogen storage. In this work, we employed kinetic analyses to demonstrate that the mechanism of hydrogen desorption depends on the sample morphology and desorption conditions. Upon the formation of Li amide bromide (Li_2NH_2Br), the $LiNH_2$ unit is confined in the cage of Br, resulting in less mobility of ion. Hydrogen desorption from the Li_2NH_2Br−2LiH system appears to follow the NH_3 mediated mechanism even if the two starting chemicals have been intensively ball milled. On the other hand, the migrations of Li^+ and H^+ play important roles leading to H_2 formation from the direct combination of H^+ (from $-NH_2$) and H^- (from LiH) when $LiNH_2$ and LiH are intimately in contact.

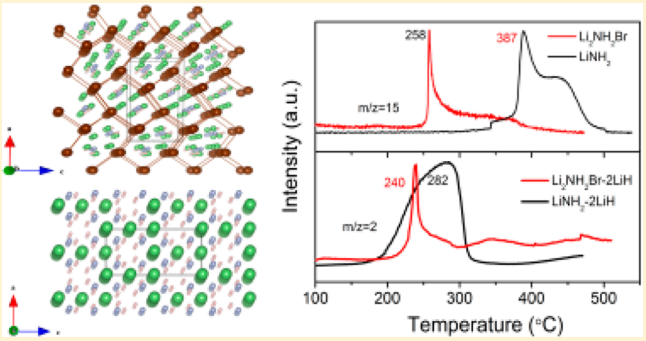

1. INTRODUCTION

There are controversial interpretations on hydrogen desorption from the amide−hydride composite hydrogen storage material,[1−14] among which the direct solid−solid reaction mechanism was proposed by Chen et al.[1,2] and the ammonia mediated mechanism was suggested by Hu[4] and Ichikawa et al.,[5,6] have been widely discussed. The experimental evidence that supports the first interpretation is the pronounced reduction in hydrogen desorption temperatures of various amide−hydride composites as compared to the decomposition temperatures of amides alone.[1,2,11] Specifically for the $Mg(NH_2)_2$−2LiH system,[15,16] the apparent activation energy of dehydrogenation is 88.1 kJ/mol, which is significantly lower than that of the thermal decomposition of $Mg(NH_2)_2$ (130 kJ/mol). Moreover, the combination of the positively charged hydrogen (H^+) in amide and negatively charged hydrogen (H^-) in hydride is energetically favored.[1−3,9,11,17] Therefore, dehydrogenation that involves a different reaction path is highly possible.[2] More recently, an in-situ TEM characterization done by Isobe et al.[3] showed that the particles of $LiNH_2$ kept essentially unchanged while LiH particles shrank upon hydrogen desorption, evidencing the immobility of N in the amide phase. The ammonia-mediated mechanism, on the other hand, constitutes two steps: first, the self-decomposition of $LiNH_2$ gives rise to Li_2NH and NH_3; second, the emitted NH_3 reacts with LiH to form H_2 and $LiNH_2$.[5] Such a mechanism is supported by the fact that NH_3 reacts spontaneously with LiH in an ultrafast manner,[4] and NH_3 byproduct is released in parallel with the evolution of H_2.[5,13] It should be pointed out that one of the characteristics of the NH_3 mediated mechanism is that part of N atoms previously position in the amide phase will be relocated to the hydride phase through the liberation of gaseous NH_3 and captured by LiH. David et al.[7] proposed a Frenkel defect pairs mechanism which is associated with the migration of both Li^+ and H^+ in amide phase and suggested that the migration of Li^+ and H^+ induces NH_3 formation, forming a series of nonstoichiometric intermediates. Wu[8] investigated the dehydrogenation of the $LiNH_2$−CaH_2 system and suggested that dehydrogenation is based on Frenkel defect pairs and the migrations of Li^+, H^+, and H^- species. It should be highlighted that all these mechanistic interpretations[1,5,7] were proposed under given circumstances, and therefore, it is worthy of depicting above-mentioned mechanisms in a more specific manner. In the present study, we focus on the $LiNH_2$−LiH

Received: November 25, 2013
Revised: January 14, 2014
Published: January 15, 2014

   dx.doi.org/10.1021/jp411551v | J. Phys. Chem. C 2014, 118, 2344−2349

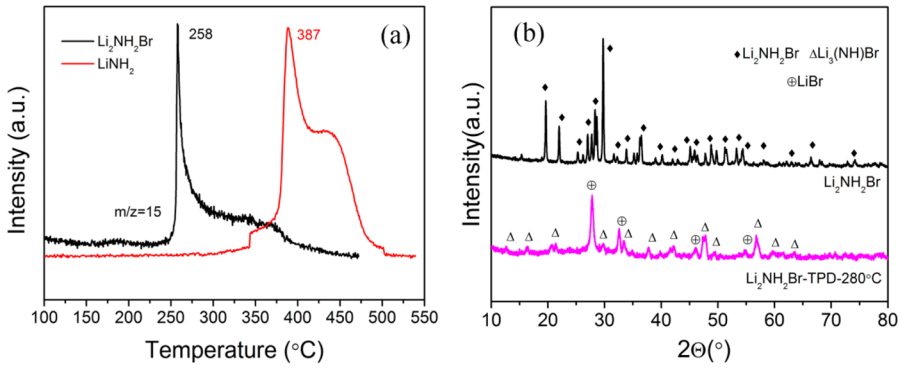

Figure 1. TPD curves of NH_3 release from as-prepared Li_2NH_2Br and raw $LiNH_2$ samples (a). XRD patterns of as-prepared Li_2NH_2Br and Li_2NH_2Br after TPD release (RS) at 280 °C (b). To avoid water vapor interference, an MS channel of m/z =15 instead of m/z =17 is used for NH_3 detection.

system[18] (see eq 1) to verify that hydrogen release follows different mechanisms under varied reaction conditions.

$$LiNH_2 + LiH \leftrightarrow Li_2NH + H_2 \quad (1)$$

In 1994, Jacobs reported that $LiNH_2$ reacts with LiBr to form Li_2NH_2Br.[19] Recently, Anderson et al.[20] found that halide-containing amides−LiH composites release hydrogen more rapidly than the neat $LiNH_2$−LiH, owing to the enhanced Li ion mobility in the halide amides. In the present study, we synthesized Li_2NH_2Br and investigated its interaction with LiH. Our results show that the rate-determining step of hydrogen desorption from the Li_2NH_2Br−2LiH system is ammonia liberating from Li_2NH_2Br with a high activation energy (E_a) of 162.1 kJ/mol. However, the E_a for hydrogen desorption from the sufficiently ball milled $LiNH_2$−2LiH sample is ca. 83.3 kJ/mol, which is about half of the self-decomposition of Li_2NH_2Br and 62.6% of the self-decomposition of $LiNH_2$. Structural analyses manifest that upon the formation of Li amide bromide (Li_2NH_2Br) $LiNH_2$ unit is caged within the Br framework. Because of the limited mobility, the caged $LiNH_2$ in the Li_2NH_2Br−2LiH system is likely to undergo a NH_3 mediated mechanism in the hydrogen desorption. On the other hand, the migrations of Li^+ and H^+ play important roles leading to H_2 formation from the direct combination of H^+ and H^- when amide and hydride are contacted sufficiently.

2. EXPERIMENTAL DETAILS

LiH (purity of 98%), LiBr (99.998%), and $LiNH_2$ (95%) were purchased from Alfa-Aesar. All chemicals were directly used without further treatment. Li_2NH_2Br was synthesized according to the literature reports[19,20] by calcining the mixture of $LiNH_2$−LiBr at 220 °C for 10 h (its XRD pattern is shown in Figure S1). Li_2NH_2Br−2LiH and $LiNH_2$−2LiH samples were prepared by ball milling (BM) the starting chemicals in an agate jar at 150 rpm for 12 h. The ball-to-sample weight ratio is about 10:1. A Retsch planetary ball mill (PM400) was employed. The samples were milled for 4 min in one direction, halted for 1 min, and revolved in the reverse direction. All samples were handled in a MBRAUN glovebox filled with high-purity argon (O_2 < 10 ppm, H_2O < 0.1 ppm) to avoid air contamination.

A 10 mg sample was loaded in an Al_2O_3 crucible for thermogravimetric measurement on a Netzsch TG-DTA apparatus (Netzsch, Germany) at a ramping rate of 4 °C/min. A temperature-programmed desorption (TPD) was performed to study the thermal decomposition properties of samples on a custom-built TPD and mass spectrometer (MS, Hiden) combined system. About 5 mg of sample was tested each time.

Activation energies with an ∼±10% of measurement errors were attained by Kissinger's method, and the fastest reaction rates were monitored by the TPD technique. Reaction rates constants (±13% of measurement errors) at different temperatures were evaluated by Kissinger's method and Arrhenius plot.

XRD measurements were conducted on a PANalytical X'pert diffractometer (Cu Kα, 40 kV, 40 mA). A self-made sample cell was used to protect the samples from air contamination. FTIR measurements were measured on a Varian 3100 FTIR spectrophotometer (Excalibar Series) in DRIFT mode (diffuse reflectance infrared Fourier transform).

3. RESULTS

3.1. Thermal Decomposition of Li_2NH_2Br and $LiNH_2$.

The TPD curves of the as-prepared Li_2NH_2Br and $LiNH_2$ samples are summarized in Figure 1a. Li_2NH_2Br started to release NH_3 at around 250 °C, peaked at 258 °C, and ended around 450 °C. LiBr and $Li_3(NH)Br$ are the solid products (see Figure1b) showing the occurrence of reaction 2.

$$2Li_2NH_2Br \rightarrow Li_3(NH)Br + LiBr + NH_3 \quad (2)$$

$LiNH_2$, on the other hand, exhibited ammonia onset and peak temperatures at 350 and 387 °C, which are more than 100 °C higher than that of Li_2NH_2Br (see Figure 1a). Nevertheless, NH_3 release from both samples exhibit some similar features, i.e., rapid increase in NH_3 concentration within a short temperature range and asymmetric NH_3 curve shape. We managed to monitor the sample morphology through a transparent reactor where sample was put under a glass window (shown in Figure S2). A clear melting phenomenon was observed in both samples upon the thermal decomposition, which explains the sharp and asymmetric NH_3 signal observed in TPD. Such experimental results show that the majority of NH_3 release from both samples is in connection with the collapse of crystal structure.

As shown in Figure 2, the total weight losses upon the complete decomposition of Li_2NH_2Br and $LiNH_2$ to 450 and 520 °C were 7.7 and 36.3 wt %, respectively. However, only ca. 0.3 and 4.1 wt % of mass losses which are equivalent to 3.9 and 11.3 mol % of ammonia were detected before the melting event for the Li_2NH_2Br and $LiNH_2$ samples, respectively. It is worthy of highlighting that the NH_3 release mechanism before and

dx.doi.org/10.1021/jp411551v | J. Phys. Chem. C 2014, 118, 2344−2349

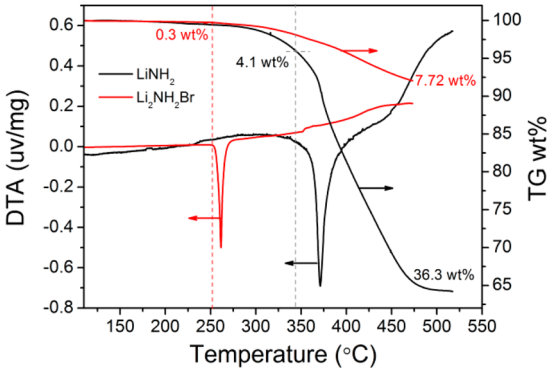

Figure 2. TG-DTA curves of NH_3 release from as-prepared Li_2NH_2Br and raw $LiNH_2$ samples.

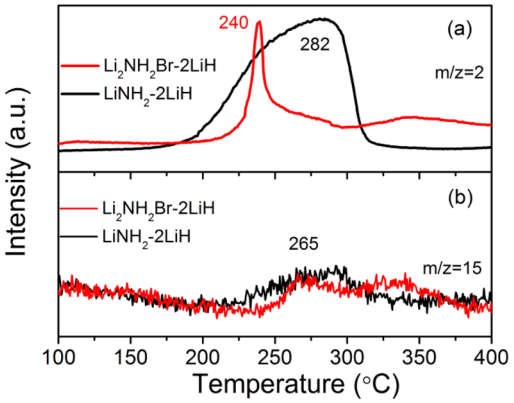

Figure 4. TPD curves of H_2 (a) and NH_3 (b) release from Li_2NH_2Br−2LiH and $LiNH_2$−2LiH samples.

after the melting of amide should be different. It is because when amide is in defined crystal structure, the cation migration which is facilitated by the Frenkel defect pairs of Li_2NH_2Br or $LiNH_2$ may account for the NH_3 formation;[7] upon melting, however, the chance of direct collision of mobile groups (such as NH_2) enhances significantly, leading to the formation of NH_3. As compared with $LiNH_2$, negligible NH_3 was detected prior to the melting of Li_2NH_2Br, indicating a remarkable different ion mobility in the structure of Li_2NH_2Br. As shown in Figure 3, the as-prepared Li_2NH_2Br is of an orthorhombic structure (*Pnma*) with a = 12.484(2) Å, b = 7.959 (1) Å, and c = 6.3851 (1) Å. In the crystal of Li_2NH_2Br, Li and NH_2 groups are within the cage of Br; the rigid lattice may somehow confine the mobility of Li and H ions even if the compound is close to its melting point. Such a phenomenon is different from the antifluoride $LiNH_2$ where cation mobility is observably high when the compound reaches ca. 3/4 of its melting point.[7,21,22] We would also like to point out that, even for $LiNH_2$ with noticeable ion conductivity prior to its melting, the rate of NH_3 release remains significantly slow (see Figure 2), and it is incompatible with the rate of hydrogen release as shown below.

3.2. H_2 from Li_2NH_2Br−2LiH and $LiNH_2$−2LiH Samples. The dehydrogenation of Li_2NH_2Br−2LiH and $LiNH_2$−2LiH samples was examined by the TPD technique. As shown in Figure 4 the H_2-TPD profile of the Li_2NH_2Br−2LiH sample (Figure 4a) resembles the NH_3-TPD profile of the neat Li_2NH_2Br sample (Figure 1a), except that the dehydrogenation peak temperature was about 20 °C lower than that of NH_3 desorption. The slightly lower temperature may be due to the faster diffusion rate of H_2 in the pipeline and the MS chamber. The dehydrogenation temperature of $LiNH_2$−2LiH, on the other hand, was more than 100 °C lower than that of $LiNH_2$ self-decomposition temperature, and the curve shape exhibits a different feature. The different profiles of H_2 and NH_3 release infer a different reaction path in H_2 desorption from Li_2NH_2Br−2LiH and $LiNH_2$−2LiH systems. To clarify the difference in the reaction path, we further carried out kinetic analyses on both systems.

Li_2NH_2Br−2LiH samples after dehydrogenation and rehydrogenation were collected for XRD and FTIR measurements. It was found that the solid residue after dehydrogenation to 280 °C contains $Li_3(NH)Br$ and LiBr phases together with the remaining excess LiH. Upon rehydrogenation at 260 °C, Li_2NH_2Br and LiH were regenerated (Figure 5a). FTIR characterization (shown in Figure 5b) also revealed the appearance of imide-like N−H stretch upon dehydrogenation and the development of the sharp stretching vibrations of N−H bond at 3284, 3245, and 3220 cm^{-1} belonging to Li_2NH_2Br upon rehydrogenation, which are in excellent agreement with the XRD data. Based on the above experimental results, the interaction between Li_2NH_2Br and LiH can be described by reaction 3.

$$Li_2NH_2Br + LiH \leftrightarrow Li_3(NH)Br + H_2 \quad (3)$$

For comparison, XRD patterns and FTIR spectra of the $LiNH_2$−2LiH sample are summarized in Figure S3.

3.3. Kinetic Analyses. Kissinger's method[2,23−25] was employed to determine the activation energy (E_a) of gas release for the Li_2NH_2Br, $LiNH_2$, Li_2NH_2Br−2LiH, and $LiNH_2$−2LiH samples. The Kissinger equation is described as follows

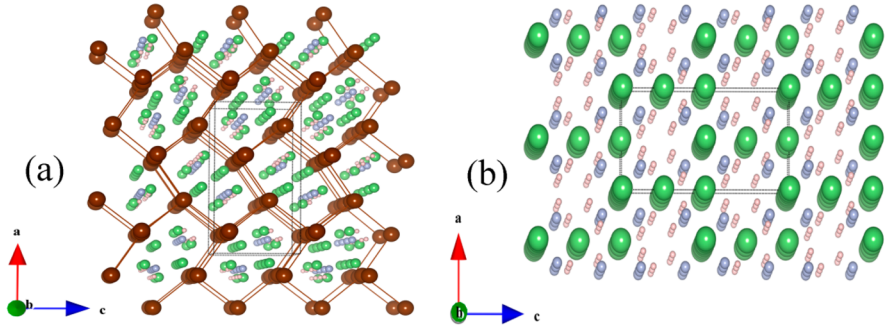

Figure 3. Crystal structures of Li_2NH_2Br[19] (010) and $LiNH_2$[28] (010). Lithium is represented by light green spheres, nitrogen by light blue spheres, hydrogen by light red spheres, and bromine by brown spheres. The unit cells are shown as dotted lines.

dx.doi.org/10.1021/jp411551v | J. Phys. Chem. C 2014, 118, 2344−2349

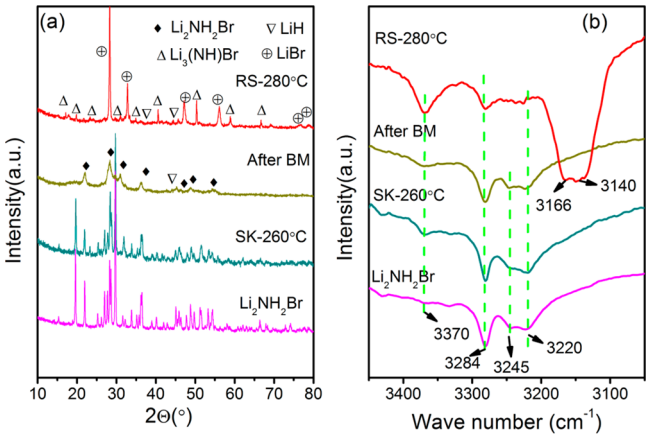

Figure 5. XRD patterns (a) and FTIR spectra (b) of the Li_2NH_2Br−2LiH system at different states: release (RS) at 280 °C, soak (SK) at 260 °C, after ball milling (BM), and as-prepared Li_2NH_2Br.

$$d[\ln(\beta/T_m^2)]/d(1/T_m)] = -E_a/R \quad (4)$$

where T_m is the peak temperature at which the maximum reaction rate is attained, β is the heating rate, E_a is the activation energy, and R is the gas constant. The TPD technique was employed to collect the maximum reaction rate temperatures at various heating rates (4, 5, 6, 7, and 8 °C/min). The dependency of $\ln(\beta/T_m^2)$ on $1/T_m$ was plotted, and the slope of the fitted line was used to determine the value of E/R.

As shown in Figure 6a,b the activation energies of self-decomposition of Li_2NH_2Br and dehydrogenation of Li_2NH_2Br−2LiH are within the error bar of the method applied[24] (162 vs 177 kJ/mol). The activation energy of post-ball-milling $LiNH_2$ sample is 133 kJ/mol (Figure 6c), which is close to the value reported by Pinkerton et al. (E_a = 128 kJ/mol).[26] The $LiNH_2$−2LiH sample, however, demonstrated a greatly reduced E_a of 83.3 kJ/mol, which is 50 kJ/mol lower than that of the decomposition of neat $LiNH_2$ (Figure 6d).

3.4. Discussion. The similarity of the E_a of NH_3 and H_2 release from Li_2NH_2Br and Li_2NH_2Br−2LiH, respectively, suggests that NH_3 formation is the rate-limiting step in H_2 release from the Li_2NH_2Br−2LiH composite. In other words, H_2 is generated following the NH_3 mediated mechanism. For $LiNH_2$−2LiH, the dehydrogenation activation energy is ca. 83.3 kJ/mol, which has a 37.4% reduction as compared to the activation energy of the self-decomposition of $LiNH_2$, showing the unlikelihood of the occurrence of NH_3 mediated reaction pathway.

The rate constants of NH_3 ($k(NH_3)$) and H_2 ($k(H_2)$) formation were further determined by the Arrhenius equation (eq 5).

$$k = A\exp(-E_a/RT) \quad (5)$$

At 220 and 250 °C, the $k(H_2)$ of Li_2NH_2Br−2LiH and the $k(NH_3)$ of Li_2NH_2Br are in the same order of magnitude, whereas for the $LiNH_2$−2LiH sample, the $k(H_2)$ are 22 and 11 times larger than those of $k(NH_3)$ of $LiNH_2$, respectively. However, it is worth to point out that at temperatures above 381 °C where $k(NH_3)$ surpasses $k(H_2)$, the NH_3 mediated pathway may be the main route for hydrogen production from the $LiNH_2$−2LiH system (as shown in Figure 7).

As clearly discussed in above section, the hydrogen desorption from the amide−hydride system is highly dependent on the sample morphology and desorption conditions. Under the following conditions when (1) the ion migration is substantially constrained as in the case of the Li_2NH_2Br−LiH composite, or (2) amide and hydride particles are not in good contact, or (3) the reaction temperature is high enough to allow NH_3 formation at a sufficient rate, hydrogen desorption is likely

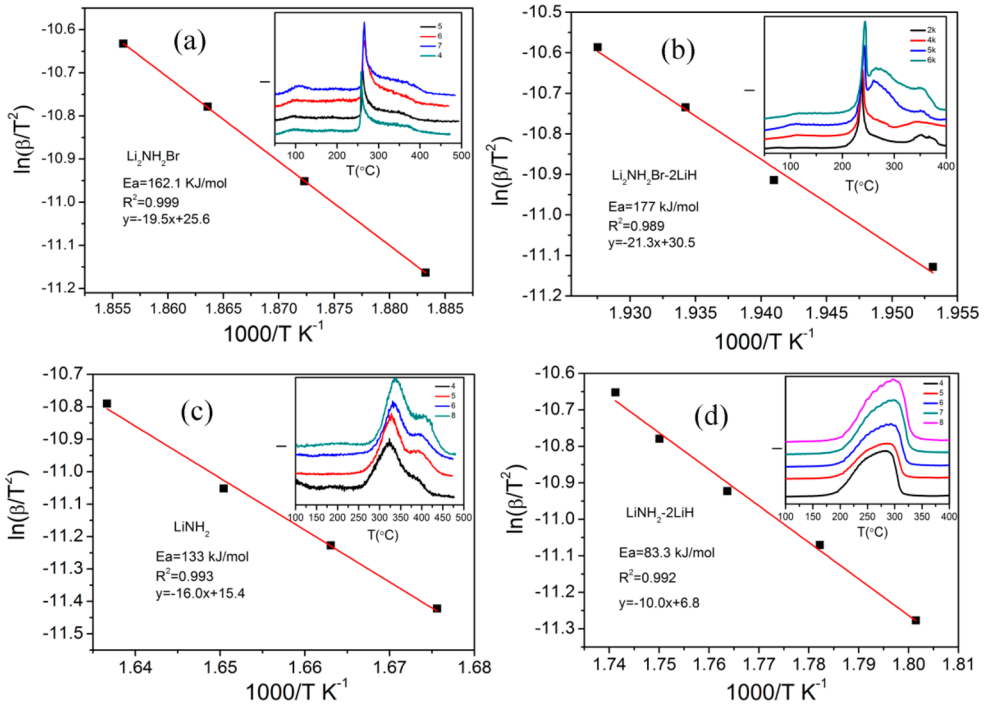

Figure 6. Kissinger's plots of Li_2NH_2Br (a), Li_2NH_2Br−2LiH (b), $LiNH_2$ (c), and $LiNH_2$−2LiH (d) samples (all samples have been ball milling for 12 h). Insets are their TPD profiles collected at different ramping rates for $LiNH_2$ (NH_3-TPD), $LiNH_2$−2LiH (H_2-TPD), Li_2NH_2Br (NH_3-TPD), and Li_2NH_2Br−2LiH (H_2-TPD).

dx.doi.org/10.1021/jp411551v | J. Phys. Chem. C 2014, 118, 2344−2349

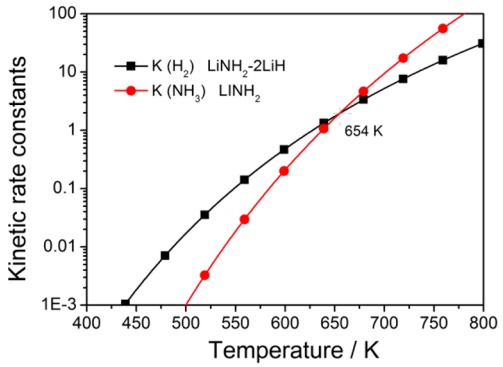

Figure 7. Kinetic rate constants against temperatures of $LiNH_2$−2LiH ($k(H_2)$) and $LiNH_2$ ($k(NH_3)$) samples.

to follow the NH_3 mediated pathway. Conversely, the reaction will follow a more energy favorable path via ion migration under mild conditions if amide and hydride particles are intimately in contact.

As for H_2 desorption from $LiNH_2$−LiH, we would like to propose a modified procedure from what suggested by Isobe et al.[3] In their model, the migration of Li^+ was of main concern. However, to realize the hydrogen release, H^+ from $LiNH_2$ should also move. Our model is illustrated in Scheme 1. H^+ from the $LiNH_2$ and Li^+ from LiH exchange at the interface of $LiNH_2$ and LiH leading to the formation of H_2 and the Li-rich layer in the amide phase. It is expected that, under such a circumstance, Li^+ and H^+ will move in an opposite direction entering and exiting the amide phase, respectively, to minimize the concentration gradient, leading to the formation of nonstoichiometric amide phase as detected by Pinkerton[26] and David.[7] The compositional change in amide phase is likely to facilitate faster Li^+ and H^+ mobility. As a matter of fact, Li_2NH has a much better Li ion conduction than $LiNH_2$.[27] With continuous exchange of H^+ and Li^+ at the interface of amide/hydride, the nonstoichiometric lithium amide/imide phase will eventually convert to lithium imide (Li_2NH).

Such a mechanism can also be applied to describe the rehydrogenation process but in a reverse manner. Upon hydrogenation, the H_2 molecule dissociates into H^+ and H^- at the surface of Li_2NH. H^- and H^+ combine with Li^+ and N to form LiH and H-rich imide on the top layer, respectively. Under such a situation, H^+ and Li^+ will move in an opposite direction entering and exiting the imide phase, respectively, to compensate for the concentration gradient, leading to the nonstoichiometric lithium amide or imide phase. With the progression of hydrogenation, LiH particle will be formed on the top of amide.

4. CONCLUSION

In this work, we employed kinetic analyses to demonstrate that the mechanism of hydrogen desorption from the amide−hydride system is highly dependent on the sample morphology and desorption conditions. Upon the formation of Li amide bromide (Li_2NH_2Br), the caging of $LiNH_2$ by the framework of Br resulted in the less mobility of ion. Therefore, hydrogen desorption from the Li_2NH_2Br−2LiH appears to follow the NH_3 mediated mechanism. Conversely, when amide and hydride are sufficiently in contact, the migrations of Li^+ and H^+ play an important role in facilitating the direct combination of H^+ ($LiNH_2$) and H^- (LiH) for H_2 formation. Overall, the direct solid−solid mechanism is viable for the dehydrogenation of the amide−hydride system that are intimately in contact. On the contrary, the ammonia mediated mechanism is well-suited for those cases when LiH and $-NH_2$ groups are unable to directly contact each other even though they are mixed in nanoscale.

■ ASSOCIATED CONTENT

Supporting Information

Characterization data and digital photographs. This material is available free of charge via the Internet at http://pubs.acs.org.

■ AUTHOR INFORMATION

Corresponding Author

*E-mail pchen@dicp.ac.cn; Tel +86-411-84379905; Fax +86-411-84685940 (P.C.).

Notes

The authors declare no competing financial interest.

■ ACKNOWLEDGMENTS

We appreciate the financial support from the National Basic Research Program of China (No. 2010CB631304), National Natural Science foundation of China (Nos. 50901070, 20971120, and 21273229), Project of National Natural Science Funds for Distinguished Young Scholar (No. 51225206), and CAS-JSPS collaborative funding.

We thank Dr. Hui Wu for her valuable comments on this paper.

■ REFERENCES

(1) Chen, P.; Xiong, Z.; Luo, J.; Lin, J.; Tan, K. L. Interaction between Lithium Amide and Lithium Hydride. *J. Phys. Chem. B* **2003**, *107*, 10967−10970.

(2) Chen, P.; Xiong, Z.; Yang, L.; Wu, G.; Luo, W. Mechanistic Investigations on the Heterogeneous Solid−State Reaction of Magnesium Amides and Lithium Hydrides. *J. Phys. Chem. B* **2006**, *110*, 14221−14225.

(3) Zhang, T.; Isobe, S.; Wang, Y.; Hashimoto, N.; Ohnuki, S. A Solid-Solid Reaction Enhanced by an Inhomogeneous Catalyst in the

Scheme 1. Schematic Illustration of the Solid−Solid Reaction Mechanism of the $LiNH_2$−LiH System

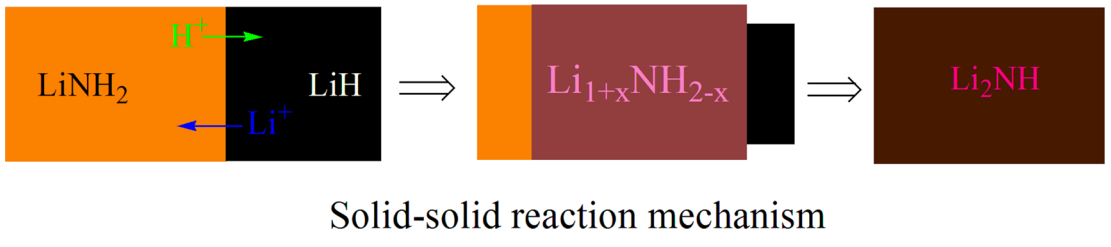

(De)hydrogenation of a Lithium−Hydrogen−Nitrogen System. *RSC Adv.* **2013**, *3*, 6311−6314.
(4) Hu, Y. H.; Ruckenstein, E. Ultrafast Reaction between LiH and NH_3 during H_2 Storage in Li_3N. *J. Phys. Chem. A* **2003**, *107*, 9737−9739.
(5) Ichikawa, T.; Hanada, N.; Isobe, S.; Leng, H.; Fujii, H. Mechanism of Novel Reaction from $LiNH_2$ and LiH to Li_2NH and H_2 as a Promising Hydrogen Storage System. *J. Phys. Chem. B* **2004**, *108*, 7887−7892.
(6) Ichikawa, T.; Hanada, N.; Isobe, S.; Leng, H. Y.; Fujii, H. Hydrogen Storage Properties in Ti Catalyzed Li−N−H system. *J. Alloys Compd.* **2005**, *404−406*, 435−438.
(7) David, W. I. F.; Jones, M. O.; Gregory, D. H.; Jewell, C. M.; Johnson, S. R.; Walton, A.; Edwards, P. P. A Mechanism for Non-stoichiometry in the Lithium Amide/Lithium Imide Hydrogen Storage Reaction. *J. Am. Chem. Soc.* **2007**, *129*, 1594−1601.
(8) Wu, H. Structure of Ternary Imide $Li_2Ca(NH)_2$ and Hydrogen Storage Mechanisms in Amide−Hydride System. *J. Am. Chem. Soc.* **2008**, *130*, 6515−6522.
(9) Aguey-Zinsou, K.-F.; Yao, J.; Guo, Z. X. Reaction Paths between $LiNH_2$ and LiH with Effects of Nitrides. *J. Phys. Chem. B* **2007**, *111*, 12531−12536.
(10) Hoang, K.; Janotti, A.; VandeWalle, C. G. The Particle-Size Dependence of the Activation Energy for Decomposition of Lithium Amide. *Angew. Chem., Int. Ed.* **2011**, *123*, 10352−10355.
(11) Lu, J.; Fang, Z. Z.; Sohn, H. Y. A Dehydrogenation Mechanism of Metal Hydrides Based on Interactions between $H^{\delta+}$ and H^-. *Inorg. Chem.* **2006**, *45*, 8749−8754.
(12) Isobe, S.; Ichikawa, T.; Hino, S.; Fujii, H. Hydrogen Desorption Mechanism in a Li−N−H System by Means of the Isotopic Exchange Technique. *J. Phys. Chem. B* **2005**, *109*, 14855−14858.
(13) Leng, H.; Ichikawa, T.; Hino, S.; Nakagawa, T.; Fujii, H. Mechanism of Hydrogenation Reaction in the Li−Mg−N−H System. *J. Phys. Chem. B* **2005**, *109*, 10744−10748.
(14) Hu, J. Z.; Kwak, J. H.; Yang, Z.; Osborn, W.; Markmaitree, T.; Shaw, L. L. Probing the Reaction Pathway of Dehydrogenation of the $LiNH_2$+LiH Mixture Using in Situ ^1H NMR Spectroscopy. *J. Power Sources* **2008**, *181*, 116−119.
(15) Luo, W. ($LiNH_2$−MgH_2): a Viable Hydrogen Storage System. *J. Alloys Compd.* **2004**, *381*, 284−287.
(16) Xiong, Z.; Wu, G.; Hu, J.; Chen, P. Ternary Imides for Hydrogen Storage. *Adv. Mater.* **2004**, *16*, 1522−1525.
(17) Grochala, W.; Edwards, P. P. Thermal Decomposition of the Non−interstitial Hydrides for the Storage and Pproduction of Hydrogen. *Chem. Rev.* **2004**, *104*, 1283−1316.
(18) Chen, P.; Xiong, Z.; Luo, J.; Lin, J.; Tan, K. L. Interaction of Hydrogen with Metal Nitrides and Imides. *Nature* **2002**, *420*, 302−304.
(19) Barlage, H.; Jacobs, H. $Li_2Br(NH_2)$: Das erste ternäre Alkalimetallamidhalogenid. *Z. Anorg. Allg. Chem.* **1994**, *620*, 479−482.
(20) Anderson, P. A.; Chater, P. A.; Hewett, D. R.; Slater, P. R. Hydrogen Storage and Ionic Mobility in Amide−Halide Systems. *Faraday Discuss.* **2011**, *151*, 271−284.
(21) Dimanov, A.; Ingrin, J. Premelting and High−Temperature Diffusion of Ca in Synthetic Diopside: An Increase of the Cation Mobility. *Phys. Chem. Miner.* **1995**, *22*, 437−442.
(22) Hayes, W.; Hutchings, M. T. *Ionic Solids at High Temperatures*; Stoneham, A. M., Ed.; World Scientific: Singapore, 1989.
(23) Matsumoto, M.; Haga, T.; Kawai, Y.; Kojima, Y. Hydrogen Desorption Reactions of Li−N−H Hydrogen Storage System:- Estimation of Activation Free Energy. *J. Alloys Compd.* **2007**, *439*, 358−362.
(24) Cao, H.; Zhang, Y.; Wang, J.; Xiong, Z.; Wu, G.; Qiu, J.; Chen, P. Effects of Al−Based Additives on the Hydrogen Storage Performance of the $Mg(NH_2)_2$−2LiH System. *Dalton Trans.* **2013**, *42*, 5524−5531.
(25) Kissinger, H. E. Reaction Kinetics in Differential Thermal Analysis. *Anal. Chem.* **1957**, *29*, 1702−1706.
(26) Pinkerton, F. E. Decomposition Kinetics of Lithium Amide for Hydrogen Storage Materials. *J. Alloys Compd.* **2005**, *400*, 76−82.
(27) Li, W.; Wu, G.; Xiong, Z.; Feng, Y. P.; Chen, P. Li^+ Ionic Conductivities and Diffusion Mechanisms in Li-Based Imides and Lithium Amide. *Phys. Chem. Chem. Phys.* **2012**, *14*, 1596−1606.
(28) Yang, J. B.; Zhou, X. D.; Cai, Q.; James, W. J.; Yelon, W. B. Crystal and Electronic Structures of $LiNH_2$. *Appl. Phys. Lett.* **2006**, *88*, 041914−041916.